Pyrazole-4-sulfonate networks of alkali and alkaline-earth metals. Effect of cation size, charge, H-bonding and aromatic interactions on the three-dimensional supramolecular architecture

Gellert Mezei and Raphael G. Raptis*

Department of Chemistry, University of Puerto Rico, P. O. Box 23346, San Juan, PR 00931-3346, USA. E-mail: raphael@adam.uprr.pr

Received (in New Haven, CT, USA) 18th March 2003, Accepted 13th May 2003
First published as an Advance Article on the web 8th August 2003

Variation of cation size and/or charge produces profound structural changes in the networks formed by pyrazole-4-sulfonate (L) with alkali and alkaline-earth metal cations. The zwitterionic ligand (HL) itself forms a robust three-dimensional H-bonded network: tetragonal $P4_2/mbc$, $a = 10.863(1)$ Å, $c = 9.195(1)$ Å, $V = 1085.0(2)$ Å^3, $Z = 8$. The Na, K, Ca and Ba salts described herein are the first structurally characterized networks formed by L. $NaL(H_2O)_2$, orthorhombic $Pbca$, $a = 9.979(3)$ Å, $b = 7.848(3)$ Å, $c = 20.583(7)$ Å, $V = 1612.0(9)$ Å, $Z = 8$; $KL(H_2O)$, orthorhombic $Pbca$, $a = 8.174(1)$ Å, $b = 8.972(1)$ Å, $c = 19.912(3)$ Å, $V = 1460.4(4)$ Å, $Z = 8$; $CaL(H_2O)_3$, triclinic $P\bar{1}$, $a = 5.9972(6)$ Å, $b = 9.2102(9)$ Å, $c = 12.957(1)$ Å, $\alpha = 76.536(2)°$, $\beta = 89.264(2)°$, $\gamma = 79.057(2)°$, $V = 683.0(1)$ Å, $Z = 2$; $BaL(H_2O)\cdot H_2O$, monoclinic $P2_1/c$, $a = 11.386(1)$ Å, $b = 4.9098(6)$ Å, $c = 24.348(3)$ Å, $\beta = 90.702(2)°$, $V = 1361.0(3)$ Å, $Z = 4$. All four metal sulfonate networks have an alternating inorganic–organic layered structure, reinforced by multiple H-bonding within the inorganic layer as well as between the organic and inorganic layers; extended π–π stacking and edge-to-face aromatic interactions within the organic layer provide further lattice strength.

Introduction

The study of extended two- and three-dimensional coordination polymers is an active area of research, due both to their interesting topological features[1,2] and potential applications as porous materials for gas storage, separation and catalysis,[3] sensors,[4] non-linear optical materials[5] and molecular-based magnets.[6] Among the increasing variety of functional coordination networks, a central place is occupied by layered metal phosphonates. These mixed inorganic–organic materials are comprised of PO_3-bridged metal centres (inorganic layer) alternating with layers containing the organic backbones. The use of different organic substituents allows the modification of the organic layer size and polarity and consequently the properties of the material.[7]

Sulfonates, RSO_3^-, which as structural analogues of phosphonates, RPO_3^{2-} (Scheme 1), also adopt layered structures in their metal salts, have received less attention due to the fact that the sulfonate group is weakly coordinating.[8–10] Indeed, while phosphonates can alone satisfy the coordination requirements of metal centres, sulfonates are often incapable of replacing coordinated water molecules.[9a,10a,d,e,11] Weak interactions, however, are source of greater coordination flexibility and ultimately of structural diversity.

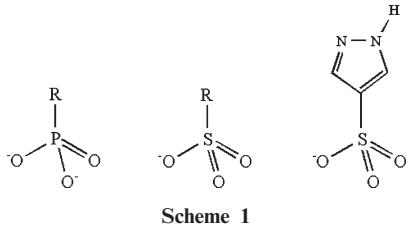

Scheme 1

The majority of studies on metal-organic coordination networks are directed towards transition metals, while alkali and alkaline-earth metals virtually fall out of interest for application purposes. Even though group-1 and -2 metals do not have some of the attractive properties of d metals (*e.g.*, redox and catalytic activity, magnetic properties), metals such as Na, K and Ca have some important advantages over transition metals. First, they are non-toxic and environmentally friendly, representing attractive green chemistry candidates. Second, their compounds are usually water soluble, eliminating the use of organic solvents for their synthesis. Finally, they are inexpensive and readily available, an important factor when it comes to large-scale applications. Consequently, those metals are attractive alternatives for the preparation of materials in which they only play a structural role. With regard to the design of functional materials based on s-metal sulfonates, the first steps have already been made: pillared, robust barium sulfonate networks have been shown to selectively adsorb H_2S[8a] and exchange Cl^- for F^- ions.[8b]

Designing and preparing novel three-dimensional networks with predetermined structure and function is not a trivial task.[12] While the relatively strong coordinate bond is widely used for the construction of coordination networks,[1–6] the emerging field of crystal engineering[13] is aiming at understanding and exploiting weak intermolecular forces, such as H-bonding,[14] halogen-bonding,[15] aromatic,[16] aurophilic[17] and other non-covalent interactions,[18] in order to assemble molecules into materials with useful properties. Our ligand of choice, pyrazole-4-sulfonate (Scheme 1), is capable of coordinating to metals through its oxygen and/or nitrogen atoms, is both a H-donor and acceptor and has a polarized π-ring susceptible for aromatic interactions.

The preparation of pyrazole-4-sulfonic acid (HL) was first reported almost fifty years ago,[19] but its solid state structure

has been hitherto unknown and its capability of forming coordination networks, as expected based on its ditopic nature, has not been explored. Calcium *N*-alkyl-pyrazole-4-sulfonates have been used as fuel and lubricant detergents and antioxidants.[20] The only reported structure containing pyrazole-4-sulfonate is that of monomeric $[Co(NH_3)_5(4\text{-}SO_3\text{-}pzH)]^{3+}$, obtained as a result of an electrophilic substitution study.[21] There are no X-ray structures reported for five-membered aromatic heterocyclic sulfonates. In this paper we describe the extended crystal structures of pyrazole-4-sulfonic acid (HL) and its four three-dimensional network structures formed with alkali and alkaline-earth metals. $NaL(H_2O)_2$, $KL(H_2O)$, $CaL_2(H_2O)_3$ and $BaL_2(H_2O)\cdot H_2O$ presented herein are the first structurally characterized networks containing pyrazole-4-sulfonate.

Results

Reaction of pyrazole-4-sulfonic acid in aqueous solution with Na_2CO_3, K_2CO_3, $CaCO_3$ and $BaCO_3$, respectively, provides the corresponding metal-sulfonate complexes, obtained as colourless crystals after water evaporation. All four complexes, as well as the free ligand, are soluble in water and DMSO but insoluble in other common organic solvents. *Ab initio* calculations suggest large dipole moments of 17 and 11 debye for zwitterionic pyrazole-4-sulfonic acid and the deprotonated ligand anion, respectively.

Description of the X-ray crystal structures

4-SO_3-pzH_2. Pyrazole-4-sulfonic acid has a zwitterionic structure, as expected for nitrogen-containing heterocycles bearing acidic groups (Fig. 1). All bond lengths and angles are within the expected ranges (Table 1). The pyrazole unit is planar (mean deviation from least-squares plane: 0.0010 Å), with a mirror plane through O1, S1, C2 bisecting the N–N bond. Both N–H hydrogen atoms of the zwitterion are involved in H-bonding with sulfonate O-atoms of two adjacent molecules (N1′···O2: 2.813(2) Å, N1″···O2: 2.857(2) Å). This is reflected in the two longer sulfur–oxygen distances of 1.452(1) Å, compared to 1.436(2) Å for the O-atom not involved in H-bonding. The charge-assisted H-bond network is responsible for the three-dimensional structure of HL (Fig. 2). The crystallographically imposed dihedral angles of 90° between the pyrazole planes define square channels along the *c*-axis, with dimensions of 4.48 × 4.48 Å.

Na(4-SO_3-pzH)(H_2O)$_2$. The Na-ion is six-coordinate, in a distorted octahedral environment, by two O-atoms from two different SO_3^- groups and four H_2O molecules (Fig. 3) (Table 2). The inorganic layer (Fig. 4) is comprised of Na-ions at distances of 3.581(2) and 4.303(1) Å from each other, bridged by

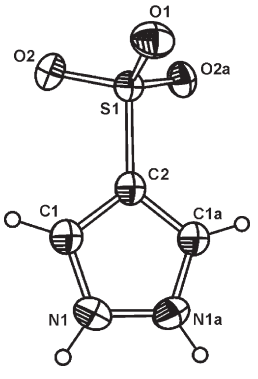

Fig. 1 Thermal ellipsoid plot (50%) of HL zwitterion. Symmetry code: ′) *x*, *y*, 2 − *z*.

Table 1 Bond lengths (Å) and angles (°) for HL

S1–O1: 1.436(2)	N1–C1: 1.322(2)
S1–O2: 1.452(1)	N1–N1a: 1.345(4)
S1–C2: 1.758(3)	C1–C2: 1.381(2)
O1–S1–O2: 113.69(7)	C1–N1–N1a: 108.96(11)
O2–S1–O2a: 112.26(11)	C1–C2–C1a: 105.9(2)
O1–S1–C2: 106.74(11)	N1–C1–C2: 108.09(18)
O2–S1–C2: 104.72(7)	C1–C2–S1: 127.05(11)

[a] Symmetry transformation used to generate equivalent atoms: a) *x*, *y*, 2 − *z*

H_2O molecules and sulfonate groups above and below the Na-layer. The H_2O molecules form intralayer H-bonds to sulfonate O-atoms (O4*···O2′: 3.047(3) Å, O4*···O3″: 2.836(2) Å, O5$^{\#}$···O1″: 2.904(2) Å) and interlayer ones to pyrazole N-atoms (O5″···N1: 2.986(3) Å). The layers are further connected by H-bonds between the other pyrazole N-atom and the non-coordinating sulfonate O-atom (N2···O3′: 2.810(3) Å) (Fig. 5). Fig. 6 depicts a perpendicular view to the organic layer, in which the pyrazole moieties are organized in a typical herringbone pattern, similar to the packing of the prototype molecule, naphthalene.[13j] Edge-to-face aromatic interactions are responsible for this pattern, with the closest contacts of H3″···C1: 2.97 Å and H1′···C2: 3.031 Å (H-centroid distances are 3.02 and 3.15 Å, respectively; dihedral angle: 65.2°).

K(4-SO_3-pzH)(H_2O). The K-ion is eight-coordinate by six O-atoms from four different SO_3^- groups and two H_2O molecules (Fig. 7) (Table 3). The structure of the inorganic layer is built on an approximately rectangular grid of K-ions (Fig. 8), with K–K separations of 4.1849(7) Å and 4.488(1) Å and K–K–K angles of 89.62 and 90.38°. Sulfonate groups cap the K_4-rectangles, while H_2O molecules bridge their longer edge. There are two H-bonds formed by the H_2O molecules: an intralayer H-bond to a sulfonate O-atom (O4′···O1: 2.854(4) Å) and an interlayer one to a pyrazole N-atom (O4*···N1: 2.972(5) Å) (Fig. 9). The pyrazole N–H hydrogen atoms form a weak, symmetrically bifurcated H-bond to a sulfonate and a water O-atom (N2···O3′: 3.066(5) Å, N2···O4″: 3.072(6) Å). In the organic layer, the pyrazole rings are organized in a

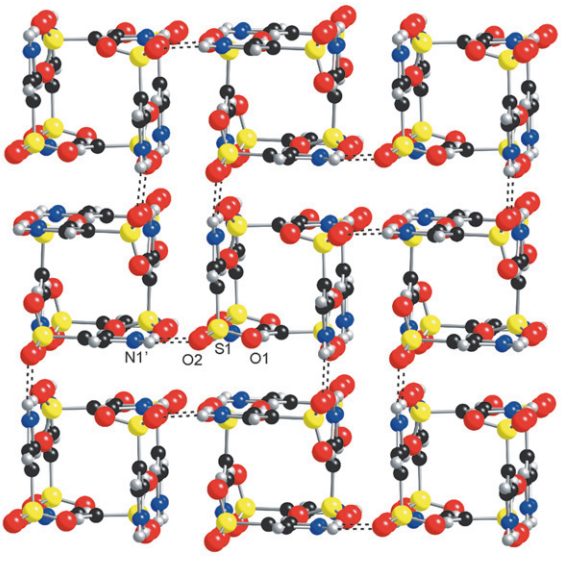

Fig. 2 Three-dimensional structure of HL, as viewed parallel to the *c*-axis. H-bonds are shown with dotted lines (the ones parallel to the *c*-axis are not shown; yellow = sulfur, red = oxygen, blue = nitrogen, black = carbon, grey = hydrogen). Symmetry code: ′) *x* + 0.5, 0.5 − *y*, *z*.

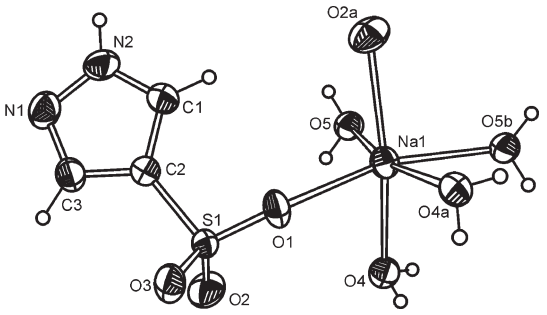

Fig. 3 Thermal ellipsoid plot (50%) of $NaL(H_2O)_2$, showing the coordination sphere around sodium. Symmetry codes: a) $0.5-x$, $y-0.5$, z; b) $-x$, $-y$, $1-z$.

typical sandwich-herringbone pattern, as in the packing of the prototype pyrene molecule.[13j] Considerably closer π–π stacking and edge-to-face aromatic interactions are observed in this case than in the Na structure (Fig. 10). The distance between the two pyrazole planes (dihedral angle: 0°, crystallographically imposed) of the "sandwich" is 3.18 Å, with a centroid–centroid distance of 3.49 Å and an angle of 24° between these two vectors. These values are typical for strong π–π stacking interactions in metal complexes with aromatic nitrogen-containing ligands.[16b] The pyrazole pairs that form the "sandwiches" are further organized in a herringbone pattern by short edge-to-face contacts, H1′···N1: 2.66 Å (H1-centroid distance: 2.94 Å; dihedral angle: 73.9°).

$Ca(4\text{-}SO_3\text{-}pzH)_2(H_2O)_3$. The Ca-ion is seven-coordinate by three O-atoms from three different SO_3^- groups, three water molecules and a pyrazole N-atom (Fig. 11) (Table 4). While still displaying a layered inorganic–organic arrangement, the structure of $CaL_2(H_2O)_3$ differs significantly from the other metal-sulfonate structures described here. Infinite ribbons along the *b*-axis (perpendicular to the direction of the inorganic layer) are locked together in the other two dimensions by multiple H-bonding to give a robust three dimensional network (Figs. 12, 13). The repeating unit of the ribbon consists of two Ca-ions bridged by two μ_2-SO_3^- groups (Ca–Ca separation: 6.026(1) Å), with the pyrazole moieties of the same ligand coordinating through their N-atom to a Ca-ion of the next unit. Each Ca-ion bears an additional terminal sulfonate group and three terminal water molecules. There is a remarkable H-bonding pattern interconnecting the infinite ribbons. In the direction of the *a*-axis (inter-ribbon Ca–Ca separation: 5.9972(6) Å), a coordinated H_2O molecule of one unit is H-bonded to the two bridging sulfonate groups of the parallel unit (O9′···O1[&]: 2.912(3) Å, O9′···O2*: 2.830(3) Å), while another H_2O molecule is H-bonded to a terminal sulfonate group (O6[#]···O8: 2.792(3) Å). In addition, the terminal ligands form H-bonds to non-coordinating N-atoms of bridging ligands through an SO_3^- oxygen atom (N2′···O4″: 2.949(3) Å) and to two H_2O molecules through their pyrazole N-atoms (N3″···O7: 2.882(3) Å, N4″···O8: 2.947(3) Å). In the direction of the *c*-axis (inter-ribbon Ca–Ca separation: 6.574(1) Å), ribbons are H-bonded through two sulfonate O-atoms of one ribbon and two H_2O molecules of the next one (O5″···O7: 2.967(3) Å, O6″···O8: 2.793(3) Å). Within the

Table 2 Selected bond lengths (Å) for $NaL(H_2O)_2$

Na1–O1: 2.362(2)	Na1–O4a: 2.463(2)	S1–O1: 1.442(2)
Na1–O2a: 2.373(2)	Na1–O5: 2.387(2)	S1–O2: 1.441(2)
Na1–O4: 2.482(2)	Na1–O5b: 2.466(2)	S1–O3: 1.459(2)

[a] Symmetry transformations used to generate equivalent atoms: a) $0.5-x$, $y-0.5$, z; b) $-x$, $-y$, $1-z$

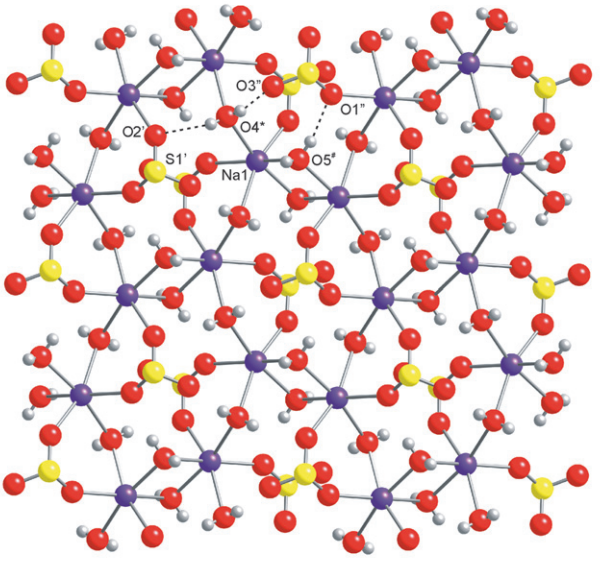

Fig. 4 View of the inorganic layer in $NaL(H_2O)_2$ parallel to the *c*-axis (pyrazole rings are not shown for clarity). Symmetry codes: ′) $-x-1$, $-y-1$, $-z$; ″) $x+0.5$, $-y-1.5$, $-z$; *) $-x-0.5$, $y-0.5$, z; [#]) $-x$, $-y-1$, $-z$.

organic layer, pyrazole groups are arranged in a brick-wall pattern, with alternating pairs of symmetry related rows (Fig. 14). Close π–π stacking, suggesting significant interactions, exists between pyrazole rings of adjacent rows; intrapair dihedral angle: 0°, interpair dihedral angle: 10.9°.

$Ba(4\text{-}SO_3\text{-}pzH)_2(H_2O)\cdot H_2O$. The Ba-ions are ten-coordinate by a pyrazole N-atom, eight O-atoms from six different SO_3^- groups and a H_2O molecule (Fig. 15) (Table 5). The three-dimensional architecture of $BaL_2(H_2O)\cdot H_2O$ can be best described as layers consisting of infinite inorganic ribbons, bridged by pyrazole-4-sulfonate ligands (Fig. 16). Within the inorganic ribbon, the Ba-ions are arranged in a ladder-shaped pattern, with Ba–Ba distances of 4.653(1) Å (across the ladder) and 4.910(1) Å (along the ladder), and Ba–Ba–Ba angles of

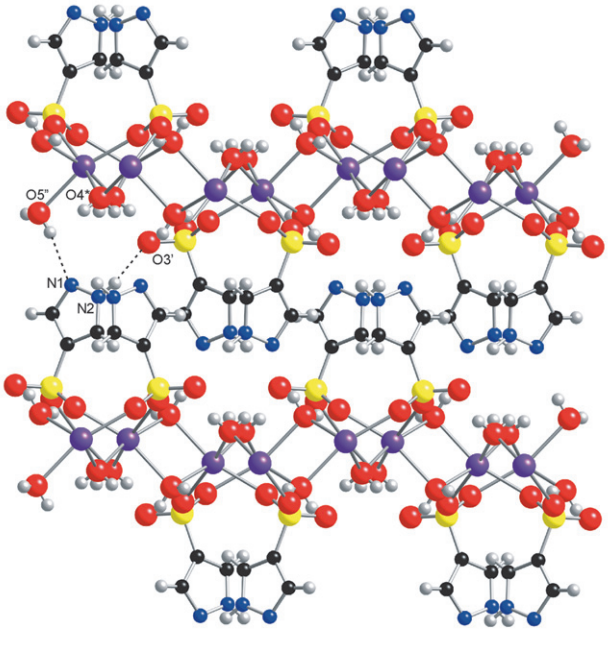

Fig. 5 View of the inorganic–organic layered structure of $NaL(H_2O)_2$ parallel to the *b*-axis. Symmetry codes: ′) $x+0.5$, y, $0.5-z$;″) $x-0.5$, y, $0.5-z$; *) $-x-1.5$, $1-y$, $z-0.5$.

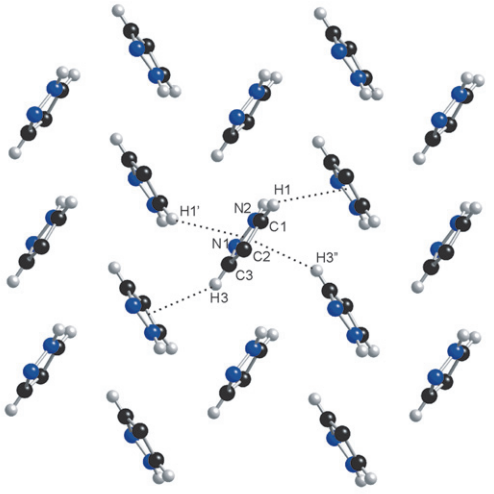

Fig. 6 Perpendicular view to the organic layer in $NaL(H_2O)_2$ (parallel to the *c*-axis), revealing the pyrazole rings organized in a herringbone pattern by edge-to-face aromatic interactions. Symmetry codes: ′) $1.5-x$, $y+0.5$, z; ″) $2-x$, $y-0.5$, $0.5-z$.

89.62 and 90.38°, respectively. The rectangles defined by two steps of the ladder are bridged on either side by a sulfonate group. The parallel ladders (Ba–Ba separation: 6.742(1) Å) are interconnected by bridging pyrazole-4-sulfonate ligands, with a N-atom coordinating to a Ba-ion of one ladder and two O-atoms of the sulfonate group to two Ba-ions of the adjacent ladder. The remaining N- and O-atoms of the bridging ligand are H-bonded to a sulfonate O-atom (N4′···O2″: 2.805(5) Å) and to a pyrazole N-atom from another layer (O5′···N2″: 2.817(5) Å), respectively. Each Ba-ion bears one terminal H_2O, which is in H-bonding distance from a sulfonate O-atom of a bridging ligand (O7···O6′: 3.045(5) Å) and a pyrazole N-atom from another layer (O7···N1″: 2.860(6) Å). Such a bonding pattern generates infinite channels parallel to the *b*-axis (Fig. 17). These channels are filled by water molecules forming a single H-bonded zig-zag file (O8*···O8$^{\#}$: 2.834(6) Å), with additional H-bonds to sulfonate O-atoms of the channel walls (O8*···O5′: 2.917(5) Å). In contrast to the previously described sulfonate structures, the inorganic and organic layers of $BaL_2(H_2O)\cdot H_2O$ are not stacked along one of the unit cell axes, but in an oblique direction (Fig. 17). Within the organic layer, the pyrazole rings are arranged in herringbone-type strips running along opposite directions (Fig. 18). Each strip consists of four rows, which are interconnected by edge-to-face aromatic interactions (closest contact/H-centroid distance/dihedral angle, H4A···C2″: 2.75 Å/3.11 Å/97.1°; H6′···C6: 2.68 Å/2.84 Å/71.4°; H1···N4: 2.80 Å/2.88 Å/82.9°). Weak π–π interactions exist between adjacent strips (distance between pyrazole planes: 3.47 Å, centroid–centroid distance: 4.91 Å).

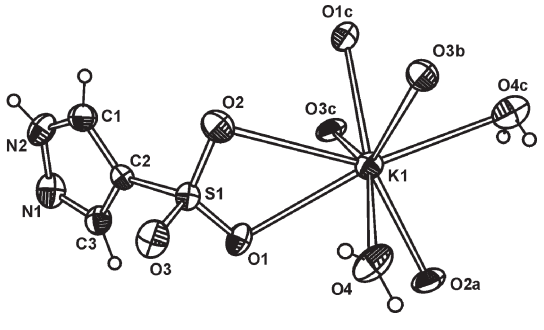

Fig. 7 Thermal ellipsoid plot (50%) of $KL(H_2O)$, showing the coordination sphere around potassium. Symmetry codes: a) $x+0.5$, y, $0.5-z$; b) $-x$, $y-0.5$, $0.5-z$; c) $0.5-x$, $y-0.5$, z.

Table 3 Selected bond lengths (Å) for $KL(H_2O)$

K1–O1: 2.828(3)	K1–O3b: 2.755(3)	S1–O1: 1.458(3)
K1–O1c: 2.810(3)	K1–O3c: 2.950(3)	S1–O2: 1.442(3)
K1–O2: 3.005(3)	K1–O4: 2.854(4)	S1–O3: 1.450(3)
K1–O2a: 2.726(3)	K1–O4c: 3.080(4)	

[a] Symmetry transformations used to generate equivalent atoms: a) $x+0.5$, y, $0.5-z$; b) $-x$, $y-0.5$, $0.5-z$; c) $0.5-x$, $y-0.5$, z

Spectral and thermogravimetric analysis

The infrared spectra of the complexes show a strong, broad absorption band with several maxima between 3550–3110 cm^{-1}, characteristic of the stretching vibrations of N–H and O–H groups involved in extensive H-bonding. The absence of bands above 3120 cm^{-1} in the spectrum of HL confirms its water-free solid state lattice determined by X-ray diffraction. C–H stretching vibrations are observed in the 3075–2930 cm^{-1} region. Bands corresponding to the vibrations of the pyrazole rings spread over the regions 1670–1380 and 1150–600 cm^{-1}. The strong bands in the 1290–1160 cm^{-1} region are attributed to vibrations of the sulfonate group.[22]

Thermogravimetric analysis (TGA) shows no weight loss for HL up to 305 °C. Above this temperature a sharp weight loss of 87% is observed up to 400 °C, then the rest of the material (100%) is lost slowly up to 560 °C.

For $NaL(H_2O)_2$, the TGA analysis shows the loss of both water molecules from 65 to 105 °C (calc. 17.5%, obs. 17.7%). In the case of $KL(H_2O)$, the loss of the H_2O molecule occurs from 70 to 105 °C (calc. 8.8%, obs. 9.0%). For $CaL(H_2O)_3$, sequential loss of water is observed: one H_2O from 70 to 100 °C (calc. 4.6%, obs. 4.2%) and two H_2O molecules from 115 to 140 °C (calc. 9.3%, obs. 9.5%). In the case of $BaL(H_2O)\cdot H_2O$, both the lattice and coordinated H_2O molecules are released in a single stage from 65 to 160 °C (calc. 7.7%, obs. 7.4%). After dehydration, the four compounds are stable up to 235, 270, 240 and 230 °C, respectively. Decomposition occurs above those temperatures, leaving behind the corresponding metal sulfates (% total loss, calc./obs.: 65/64, 57/53, 65/64, 50/50).

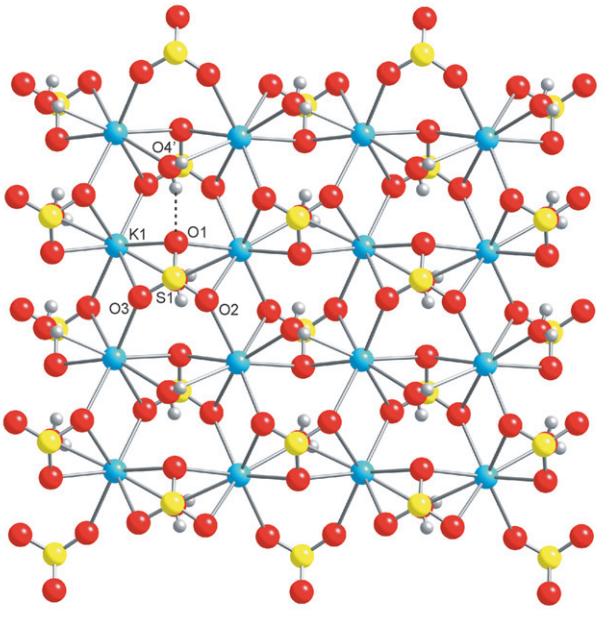

Fig. 8 View of the inorganic layer in $KL(H_2O)$ parallel to the *c*-axis (pyrazole rings are not shown for clarity). Symmetry code: ′) $x-0.5$, y, $1.5-z$.

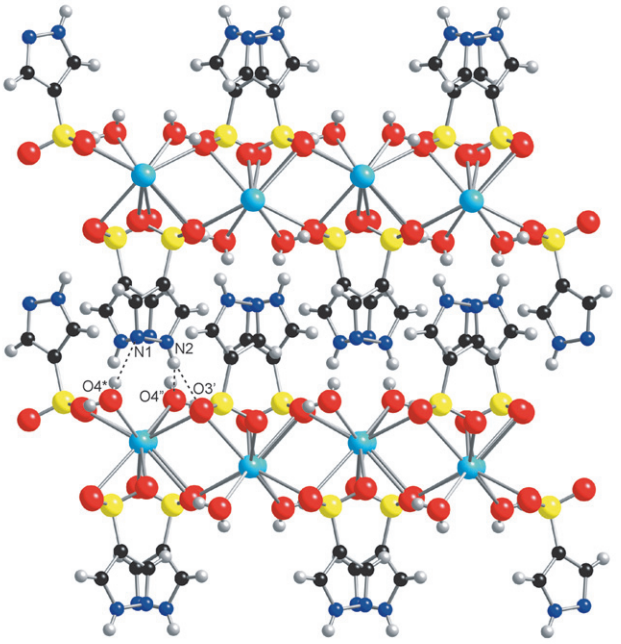

Fig. 9 View of the inorganic–organic layered structure of $KL(H_2O)$ parallel to the *b*-axis. Symmetry codes: ′) $-x$, $1-y$, $1-z$; ″) x, $0.5-y$, $z+0.5$; *) $0.5-x$, $1-y$, $z+0.5$.

Discussion

The large dipole moment and the extended H-bond network of the zwitterionic pyrazole-4-sulfonic acid induces an efficient packing in the solid state, reflected in its high density of 1.814 g cm^{-3}. Changing the most acidic proton for a cation disrupts the close-packing of the ligand molecules and the resulting salts adopt layered structures, with marked structural differences allowed by the weak coordinating capability of the sulfonate group and the uptake of varying amounts of water.

The coordination number around the cations increases with both their ionic radius and charge (Table 6). With the smaller cations, Na^+ and Ca^{2+}, the sulfonate group displays either a terminal or a μ_2-bridging coordination mode, while in the case of the larger K^+ and Ba^{2+} cations μ_2- and μ_4-bridging modes

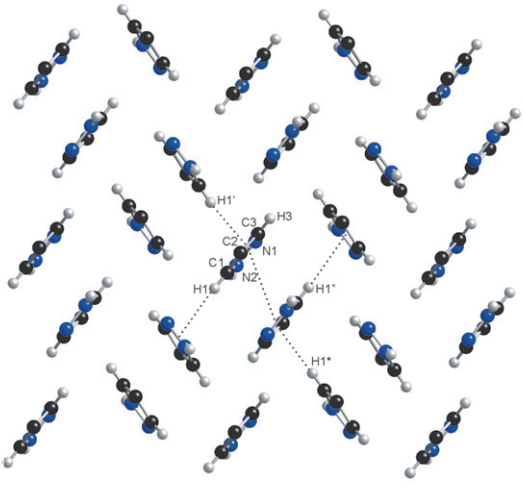

Fig. 10 Perpendicular view to the organic layer in $KL(H_2O)$ (parallel to the *c*-axis), revealing the pyrazole rings organized in a sandwich-herringbone pattern by π–π stacking and edge-to-face aromatic interactions. Symmetry codes: ′) $x+0.5$, $0.5-y$, $1-z$; ″) $2-x$, $1-y$, $1-z$; *) $1.5-x$, $y+0.5$, z.

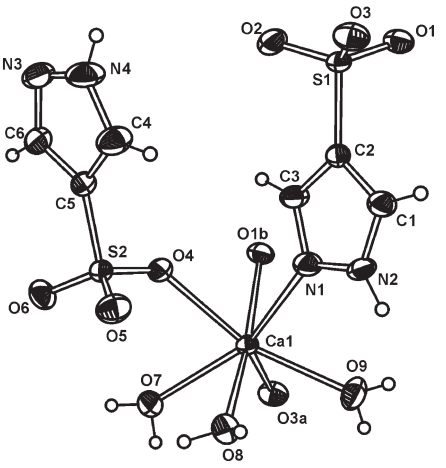

Fig. 11 Thermal ellipsoid plot (50%) of $CaL_2(H_2O)_3$, showing the coordination sphere around calcium. Symmetry codes: a) $-x$, $1-y$, $1-z$; b) $1-x$, $1-y$, $1-z$; c) $2-x$, $1-y$, $1-z$; d) x, $y+1$, z.

are observed (Scheme 2). In the latter case the sulfonate group displays also a chelating mode. The number of coordinated H_2O molecules decreases with increasing cation size and increasing hapticity of the sulfonate ligand. The pyrazole group is only coordinating to the cations with higher charge, Ca^{2+} and Ba^{2+}.

The three-dimensional, layered structures of all four salts incorporate two types of weak forces: H-bonding[14] and aromatic interactions.[16,24] The pyrazole moiety is recognized as a particularly useful synthon for organization at the supramolecular level, as it participates both as donor and acceptor in the H-bond network. Within the organic layer, pyrazole rings stemming from two adjacent inorganic layers are further connected by π–π stacking and edge-to-face aromatic interactions. Moreover, pyrazole-4-sulfonate acts as pillar between the inorganic layers of the Ca salt at a distance of 8.96 Å, while larger separations of 9.93, 9.96 and 10.29 Å are observed in the case of the Ba, K and Na salts, respectively (distances are measured between centres of consecutive inorganic layers). The order of interlayer M–M separation, Ca < Ba < K < Na, is the opposite to the order of the shortest intralayer M–M distances, Na (3.58 Å) < K (4.18 Å) < Ba (4.65 Å) < Ca (6.00 Å). Remarkably, all oxygen, nitrogen and N–H, O–H hydrogen atoms participate in the construction of the three-dimensional architecture.

The structures of the pyrazole-sulfonate networks described herein are similar to the ones reported for related sulfonates and phosphonates, in that they all form alternating inorganic and organic layers. On the other hand, the presence of the pyrazole groups render both the inorganic layer and the overall three-dimensional structures unique. The structure of the inorganic layer, and implicitly of the organic one, is primarily determined by the nature of the metal ion. A small modification of the organic group, however, induces a significant change in the structure of the inorganic layer: changing a hydroxo to an amino group in the organic backbone of a sulfonated azo-dye salt, for example, changes the coordination

Table 4 Selected bond lengths (Å) for $CaL_2(H_2O)_3$

Ca1–O1: 2.408(2)	Ca1–O9: 2.371(2)	S2–O4: 1.471(2)
Ca1–O3: 2.398(2)	Ca1–N1: 2.593(2)	S2–O5: 1.438(2)
Ca1–O4: 2.399(2)	S1b–O1c: 1.468(2)	S2–O6: 1.451(2)
Ca1–O7: 2.456(2)	S1b–O2c: 1.442(2)	
Ca1–O8: 2.405(2)	S1b–O3d: 1.444(2)	

[a] Symmetry transformations used to generate equivalent atoms: a) $-x$, $1-y$, $1-z$; b) $1-x$, $1-y$, $1-z$; c) $2-x$, $1-y$, $1-z$; d) x, $1+y$, z

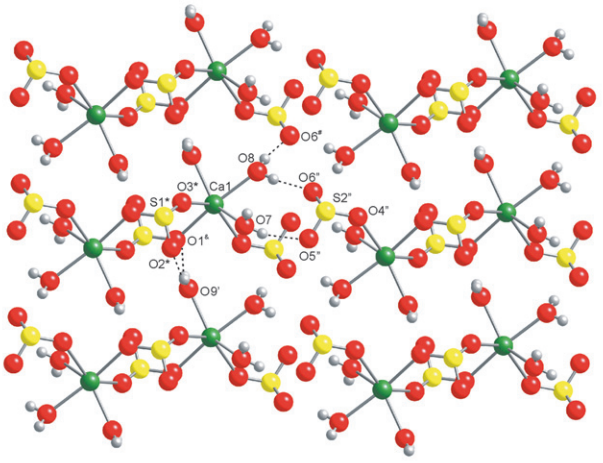

Fig. 12 View of the inorganic layer in $CaL_2(H_2O)_3$ parallel to the *b*-axis (pyrazole rings are not shown for clarity). Symmetry codes: ′) $x+1, y, z$; ″) $2-x, 2-y, 2-z$; *) $x, y+1, z$; #) $x-1, y, z$; &) $2-x, 1-y, 3-z$.

mode of the sulfonate from μ_3 to μ_2 in the case of the Na-salt and from μ_2 to terminal in the case of the Ca-salt.[25] This is allowed by the coordination flexibility of the sulfonate group, which adopts different coordination modes depending on the attached organic group and the metal ion. While μ_2-, μ_3- and μ_4-modes are all frequent in sodium sulfonate structures, the majority of the K structures contain μ_4-sulfonate groups. In the case of doubly charged Ca^{2+}, the two charge-balancing sulfonate ligands are usually μ_2-bridging or terminal. For the larger Ba^{2+} cation terminal and μ_2- to μ_4-bridging modes have been reported (a Cambridge Structural Database[26] search shows 93, 53, 16 and 8 relevant Na, K, Ca and Ba-sulfonate structures, respectively). In most cases, as in the present case, the coordination sphere around the cations is completed by H_2O molecules, whose decreasing number is correlated with the increasing hapticity of the sulfonate ligand.

The present study demonstrates the architectural effects induced by variations of ionic radii and charge, on the three-dimensional structure of pyrazole-4-sulfonate networks. We are currently extending this work to other main-group and transition series metals.

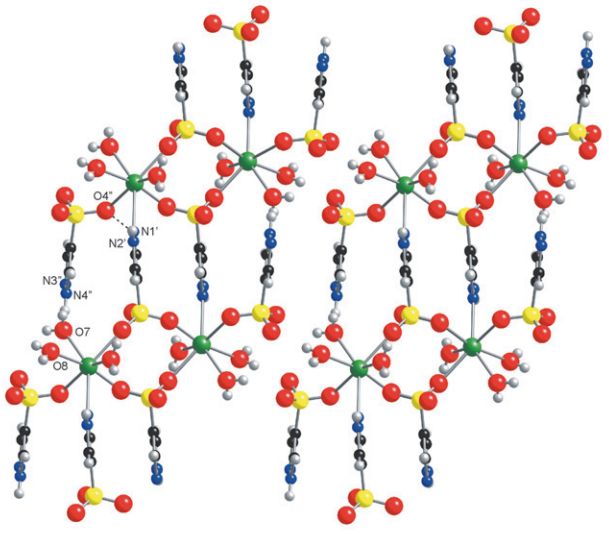

Fig. 13 View of the inorganic–organic layered structure of $CaL_2(H_2O)_3$ parallel to the *a*-axis. Symmetry codes: ′) $x, y+1, z$; ″) $x-1, y+1, z$.

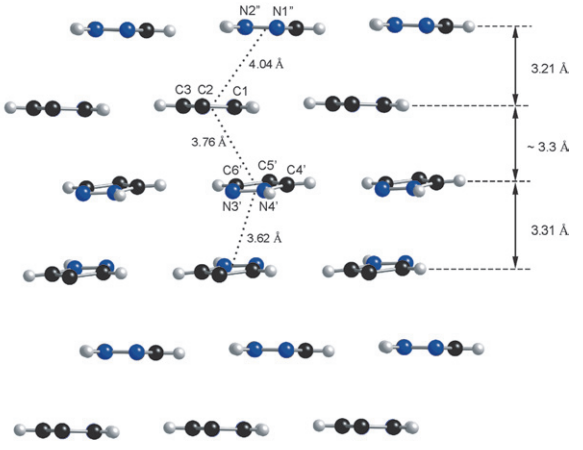

Fig. 14 Perpendicular view to the organic layer in $CaL_2(H_2O)_3$ (parallel to the *b*-axis), revealing the pyrazole rings organized in a brick-wall pattern by π–π stacking interactions. Symmetry codes: ′) $x+1, y, z$; ″) $1-x, 1-y, 1-z$.

Experimental

Materials and methods

All commercially available reagents are used as received. Elemental analyses are performed by Galbraith Laboratories, Inc., Knoxville, TN. Infrared spectra are recorded on a Nicolet FT-IR 6000 in KBr pellets. TGA data are obtained on a Shimadzu TGA-50 analyser, heated at 5 °C min^{-1} from 25 to 600 °C under air. Dipole moment calculations are performed with PC Spartan Pro (Wavefunction, Inc., 1999) at the Hartree–Fock level using the 6-31G** basis set.

X-ray diffraction data, collected at room temperature (298–301 K) from a single crystal mounted atop a glass fibre with a Siemens SMART-CCD diffractometer,[27a] are corrected for Lorentz and polarization effects.[27b] The structures are solved employing the SHELXTL-direct methods program and refined by full-matrix least-squares methods on F^2.[27c] Crystallographic details are summarized in Table 7.

CCDC reference numbers 201504–201508. See http://www.rsc.org/suppdata/nj/b3/b303096b/ for crystallographic files in .cif or other electronic format.

Synthesis and characterization

Pyrazole-4-sulfonic acid (HL) is prepared according to a literature method[19] by sulfonation of pyrazole with excess oleum

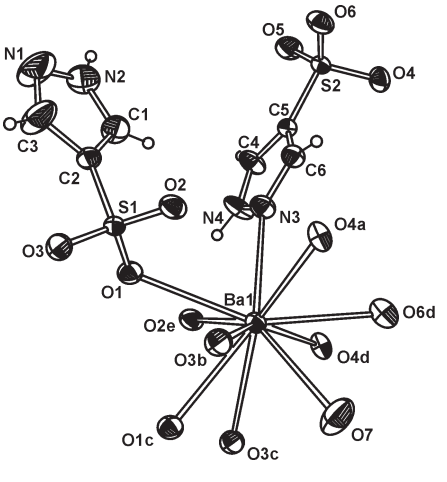

Fig. 15 Thermal ellipsoid plot (50%) of $BaL_2(H_2O)\cdot H_2O$, showing the coordination sphere around barium. Symmetry codes: a) $x, y-1, z$; b) $2-x, 2-y, 1-z$; c) $x, y+1, z$; d) $2-x, 1-y, 1-z$; e) $-x, y+0.5, 1.5-z$.

Table 5 Selected bond lengths (Å) for $BaL_2(H_2O)\cdot H_2O$

Ba1–O1: 2.890(3)	Ba1–O4: 3.053(3)	S1–O1: 1.460(3)
Ba1–O1b: 2.872(3)	Ba1–O4a: 2.786(3)	S1–O2: 1.457(3)
Ba1–O2c: 2.910(3)	Ba1–O6: 2.899(3)	S1–O3d: 1.451(3)
Ba1–O3: 2.826(3)	Ba1–O7: 2.785(4)	S2e–O4e: 1.456(3)
Ba1–O3c: 3.177(3)	Ba1–N3: 2.910(4)	S2e–O5e: 1.441(3)
		S2e–O6e: 1.451(3)

[a] Symmetry transformations used to generate equivalent atoms: a) x, $y-1$, z; b) $2-x$, $2-y$, $1-z$; c) x, $y+1$, z; d) $2-x$, $1-y$, $1-z$; e) $-x$, $y+0.5$, $1.5-z$

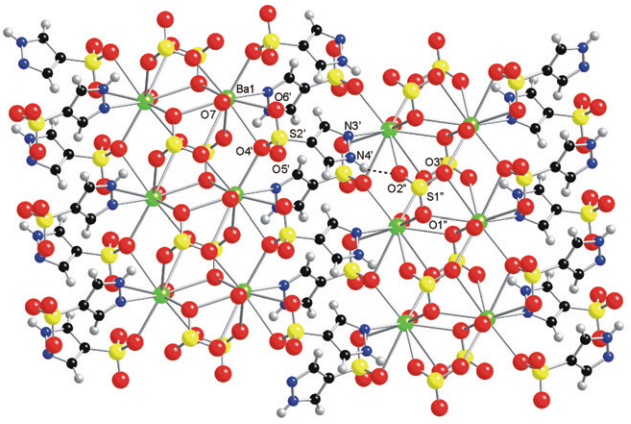

Fig. 16 View of the inorganic layer in $BaL_2(H_2O)\cdot H_2O$ parallel to the a-axis (pyrazole rings perpendicular to this layer are not shown for clarity). Symmetry codes: ′) $-x$, $y-0.5$, $1.5-z$; ″) $-x$, $y-1.5$, $1.5-z$.

(20% SO_3). The product is separated from the excess H_2SO_4 *via* its water-soluble Ba salt and recrystallized from hot water (X-ray quality crystals). Dissolution of HL and the corresponding alkali or alkaline-earth carbonates (in the required molar ratios) in H_2O provides the Na, K and Ca complexes in quantitative yield after removal of the solvent. The Ba complex is isolated as an intermediate during the synthesis of ligand HL. Colourless crystals suitable for X-ray diffraction study are obtained by slow evaporation of aqueous solutions; the Ba complex also crystallizes by layering a concentrated aqueous solution with ethanol.

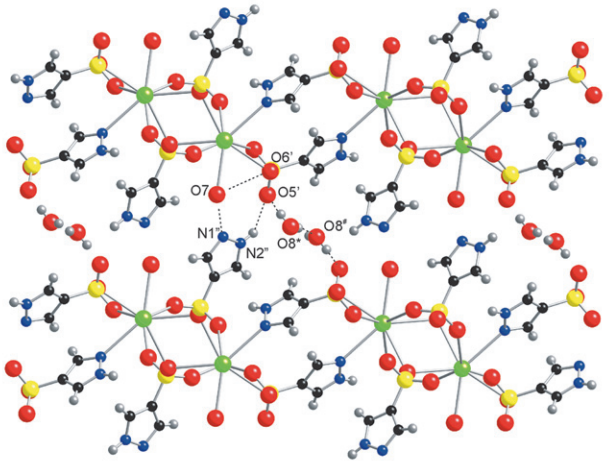

Fig. 17 View of the inorganic–organic layered structure of $BaL_2(H_2O)\cdot H_2O$ parallel to the b-axis. H atoms for O7 could not be located. Symmetry codes: ′) $2-x$, $y-0.5$, $1.5-z$; ″) $x-1$, $y-1$, z; *) $2-x$, $2-y$, $1-z$; #) $x-1$, $1.5-y$, $z+0.5$.

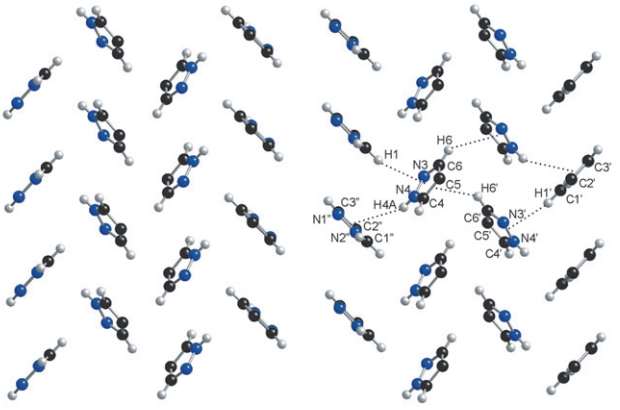

Fig. 18 View of the organic layer in $BaL_2(H_2O)\cdot H_2O$. Symmetry codes: ′) $-x$, $y+0.5$, $2.5-z$; ″) x, $y+1$, z.

Table 6 Ionic radii and coordination parameters for $NaL(H_2O)_2$, $KL(H_2O)$, $CaL_2(H_2O)_3$ and $BaL_2(H_2O)\cdot H_2O$

Cation	Ionic radius[a] /Å	Coordination number	Number of coordinated H_2O molecules	Sulfonate coordination mode
Na^+	1.02	6	4	μ_2
K^+	1.51	8	2	μ_4
Ca^{2+}	1.06	7	3	μ_2 and η^1
Ba^{2+}	1.52	10	1	μ_4 and μ_2

[a] Effective ionic radii correspond to the observed coordination numbers[23]

HL. IR (KBr, cm^{-1}): 3120 vs, 3052 vs, 2879 s, 2809 s, 2733 m, 2657 m, 1812 w, 1701 w, 1554 m, 1459 m, 1388 m, 1315 w, 1274 m, 1248 vs, 1235 vs, 1192 vs, 1088 vs, 1047 vs, 957 vs, 906 s, 898 s, 802 vs, 667 vs, 650 vs, 557 vs.

$NaL(H_2O)_2$. For $C_3H_7N_2NaO_5S$, calculated/found: C, 17.47/17.59%; H, 3.43/3.59%; N, 13.59/13.62%. IR (KBr, cm^{-1}): 3546 vs, 3488 vs, 3425 vs, 3293 s, 3206 vs, 3122 s, 3114 s, 3066 m, 2995 m, 2934 m, 1739 w, 1665 s, 1633 s, 1547 m, 1536 m, 1477 s, 1384 s, 1286 s, 1241 vs, 1201 vs, 1139 s, 1070 vs, 1057 vs, 968 s, 940 s, 871 vs, 779 s, 664 vs, 630 s, 559 s, 546 s, 497 s.

$KL(H_2O)$. For $C_3H_5KN_2O_4S$, calculated/found: C, 17.64/17.67%; H, 2.47/2.46%; N, 13.72/13.74%. IR (KBr, cm^{-1}): 3466 vs, 3395 vs, 3308 s, 3136 s, 3125 s, 3075 w, 3013 w,

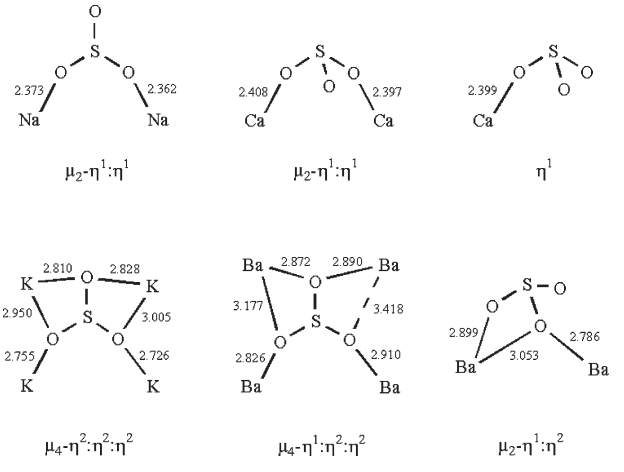

μ_2-η^1:η^1 μ_2-η^1:η^1 η^1

μ_4-η^2:η^2:η^2 μ_4-η^1:η^2:η^2 μ_2-η^1:η^2

Scheme 2 Sulfonate coordination modes (this work).

Table 7 Summary of crystallographic data

	HL	$NaL(H_2O)_2$	$KL(H_2O)$	$CaL_2(H_2O)_3$	$BaL_2(H_2O)\cdot H_2O$
Formula	$C_3H_4N_2O_3S$	$C_3H_7N_2NaO_5S$	$C_3H_5KN_2O_4S$	$C_6H_{12}CaN_4O_9S_2$	$C_6H_{10}BaN_4O_8S_2$
Formula weight	148.14	206.16	204.25	388.40	467.64
Crystal system	Tetragonal	Orthorhombic	Orthorhombic	Triclinic	Monoclinic
Space group	$P4_2/mbc$ (No. 135)	$Pbca$ (No. 61)	$Pbca$ (No. 61)	$P\bar{1}$ (No. 2)	$P2_1/c$ (No. 14)
a/Å	10.863(1)	9.979(3)	8.174(1)	5.9972(6)	11.386(1)
b/Å	10.863(1)	7.848(3)	8.972(1)	9.2102(9)	4.9098(6)
c/Å	9.195(1)	20.583(7)	19.912(3)	12.957(1)	24.348(3)
α/°	90	90	90	76.536(2)	90
β/°	90	90	90	89.264(2)	90.702(2)
γ/°	90	90	90	79.057(2)	90
V/Å^3	1085.0(2)	1612.0(9)	1460.4(4)	683.0(1)	1361.0(3)
Z	8	8	8	2	4
D_{calc}/g cm^{-3}	1.814	1.699	1.858	1.889	2.282
μ/mm^{-1}	0.520	0.441	0.980	0.820	3.270
Reflections collected/unique	4250/417	6373/1163	5775/1047	3005/1965	5491/1966
Observed reflections ($I > 2\sigma(I)$)	395	1101	864	1833	1779
$R(F)$; $Rw(F)$ ($I > 2\sigma(I)$)	0.0241; 0.0679	0.0318; 0.0841	0.0568; 0.1464	0.0330; 0.0917	0.0217; 0.0754

2959 w, 1707 w, 1646 m, 1547 w, 1487 m, 1392 m, 1328 w, 1298 m, 1218 vs, 1199 vs, 1145 s, 1062 vs, 969 s, 945 w, 879 s, 859 w, 669 vs, 607 s, 558 s, 543 s, 523 s.

$CaL(H_2O)_3$. For $C_6H_{12}CaN_4O_9S_2$, calculated/found: C, 18.55/18.69%; H, 3.12/3.18%; N, 14.43/14.43%. IR (KBr, cm^{-1}): 3507 vs, 3460 vs, 3411 vs, 3275 vs, 3144 s, 3107 s, 3082 m, 3018 m, 2962 m, 1719 w, 1663 s, 1545 m, 1490 m, 1480 m, 1399 s, 1344 m, 1301 s, 1287 s, 1246 vs, 1199 vs, 1164 vs, 1066 vs, 1051 vs, 970 vs, 953 s, 944 s, 897 m, 874 s, 858 m, 800 s, 719 s, 652 vs, 621 vs, 562 s, 544 s, 521 s, 405 m.

$BaL(H_2O)\cdot H_2O$. For $C_6H_{10}BaN_4O_8S_2$, calculated/found: C, 15.41/15.42%; H, 2.16/2.10%; N, 11.98/12.43%. IR (KBr, cm^{-1}): 3549 s, 3314 vs, 3270 vs, 3146 s, 3135 s, 3117 s, 2997 w, 2934 w, 1654 m, 1534 w, 1474 w, 1384 s, 1344 w, 1286 m, 1230 vs, 1188 vs, 1163 vs, 1065 s, 970 s, 964 s, 939 s, 906 m, 890 m, 876 w, 852 w, 787 w, 739 m, 678 s, 656 vs, 630 s, 572 s, 544 m.

Acknowledgements

G. M. acknowledges a doctoral fellowship from NSF-EPSCoR (Grant No. EPS-9874782).

References

1 Recent reviews: B. Moulton and M. J. Zaworotko, *Chem. Rev.*, 2001, **101**, 1629–1658; R. Robson, *J. Chem. Soc., Dalton Trans.*, 2000, 3735–3744; P. J. Hagrman, D. Hagrman and J. Zubieta, *Angew. Chem., Int. Ed.*, 1999, **38**, 2638–2684; A. J. Blake, N. R. Champness, P. Hubberstey, W.-S. Li, M. A. Withersby and M. Schröder, *Coord. Chem. Rev.*, 1999, **183**, 117–138; S. R. Batten and R. Robson, *Angew. Chem., Int. Ed. Engl.*, 1998, **37**, 1460–1494.

2 N. S. Oxtoby, A. J. Blake, N. R. Champness and C. Wilson, *Proc. Natl. Acad. Sci. USA*, 2002, **99**, 4905–4910; K. Biradha and M. Fujita, *Angew. Chem., Int. Ed.*, 2002, **41**, 3392–3398; K. Biradha and M. Fujita, *Chem. Commun.*, 2002, 1866; G.-F. Liu, B.-H. Ye, Y.-H. Ling and X.-M. Chen, *Chem. Commun.*, 2002, 1442–1443; O.-S. Jung, Y. J. Kim, K. M. Kim and Y.-A. Lee, *J. Am. Chem. Soc.*, 2002, **124**, 7906–7907; L. Carlucci, G. Ciani, D. M. Proserpio and S. Rizzato, *Chem. Eur. J.*, 2002, **8**, 1519–1526; E. Lee, J. Kim, J. Heo, D. Whang and K. Kim, *Angew. Chem., Int. Ed.*, 2001, **40**, 399–402; L. Carlucci, G. Ciani, D. M. Proserpio and S. Rizzato, *Chem. Commun.*, 2001, 1198–1199; A. J. Blake, N. R. Brooks, N. R. Champness, M. Crew, A. Deveson, D. Fenske, D. H. Gregory, L. R. Hanton, P. Hubberstey and M. Schröder, *Chem. Commun.*, 2001, 1432–1433; F. Mathevet and D. Luneau, *J. Am. Chem. Soc.*, 2001, **123**, 7465–7466; M. A. Withersby, A. J. Blake, N. R. Champness, P. A. Cooke, P. Hubberstey and M. Schröder, *J. Am. Chem. Soc.*, 2000, **122**, 4044–4046.

3 M. Eddaoudi, J. Kim, N. Rosi, D. Vodak, J. Wachter, M. O'Keeffe and O. M. Yaghi, *Science*, 2002, **295**, 469–472; M. E. Davis, *Nature*, 2002, **417**, 813–821; B. Chen, M. Eddaoudi, S. T. Hyde, M. O'Keeffe and O. M. Yaghi, *Science*, 2001, **291**, 1021–1023; M. Eddaoudi, D. B. Moler, H. Li, B. Chen, T. M. Reineke, M. O'Keeffe and O. M. Yaghi, *Acc. Chem. Res.*, 2001, **34**, 319–330; H. Li, M. Eddaoudi, M. O'Keeffe and O. M. Yaghi, *Nature*, 1999, **402**, 276–279; J. S. Seo, D. Whang, H. Lee, S. I. Jun, J. Oh, Y. J. Jeon and K. Kim, *Nature*, 2000, **404**, 982–986; S. S.-Y. Chui, S. M.-F. Lo, J. P. H. Charmant, A. G. Orpen and I. D. Williams, *Science*, 1999, **283**, 1148–1150; C. Janiak, *Angew. Chem., Int. Ed. Engl.*, 1997, **36**, 1431–1434; K. Uemura, S. Kitagawa, M. Kondo, K. Fukui, R. Kitaura, H.-C. Chang and T. Mizutani, *Chem. Eur. J.*, 2002, **8**, 3587–3600; C. Serre, F. Millange, C. Thouvenot, M. Noguès, G. Marsolier, D. Louër and G. Férey, *J. Am. Chem. Soc.*, 2002, **124**, 13 519–13 526.

4 G. J. Halder, C. J. Kepert, B. Moubaraki, K. S. Murray and J. D. Cashion, *Science*, 2002, **298**, 1762–1765.

5 O. R. Evans and W. Lin, *Acc. Chem. Res.*, 2002, **35**, 511–522.

6 H. O. Stumpf, L. Ouahab, Y. Pei, D. Grandjean and O. Kahn, *Science*, 1993, **261**, 447–449; O. Kahn, J. Larionova and J. V. Yakhmi, *Chem. Eur. J.*, 1999, **5**, 3443–3449.

7 A. Clearfield and Z. Wang, *Dalton Trans.*, 2002, 2937–2947; A. Clearfield, *Progr. Inorg. Chem.*, 1998, **47**, 371–510; T. E. Mallouk and J. A. Gavin, *Acc. Chem. Res.*, 1998, **31**, 209–217; M. E. Thompson, *Chem. Mater.*, 1994, **6**, 1168–1175; G. Cao, H.-G. Hong and T. E. Mallouk, *Acc. Chem. Res.*, 1992, **25**, 420–427; G. Alberti, in *Comprehensive Supramolecular Chemistry*, eds. J. L. Atwood, J. E. D. Davies, D. D. MacNicol and F. Vögtle, Elsevier Science, New York, 1996, vol. 7, pp. 151–187.

8 (*a*) A. P. Côté and G. K. H. Shimizu, *Chem. Commun.*, 2001, 251–252; (*b*) S. A. Dalrymple and G. K. H. Shimizu, *Chem. Eur. J.*, 2002, **8**, 3010–3015; (*c*) S. A. Dalrymple and G. K. H. Shimizu, *Chem. Commun.*, 2002, 2224–2225; (*d*) B. D. Chandler, A. P. Côté, D. T. Cramb, J. M. Hill and G. K. H. Shimizu, *Chem. Commun.*, 2002, 1900–1901; (*e*) S. A. Dalrymple, M. Parvez and G. K. H. Shimizu, *Chem. Commun.*, 2001, 2672–2673; (*f*) A. P. Côté, M. J. Ferguson, K. A. Khan, G. D. Enright, A. D. Kulynych, S. A. Dalrymple and G. K. H. Shimizu, *Inorg. Chem.*, 2002, **41**, 287–292; (*g*) S. A. Dalrymple, M. Parvez and G. K. H. Shimizu, *Inorg. Chem.*, 2002, **41**, 6986–6996; (*h*) J. O. Yu, A. P. Côté, G. D. Enright and G. K. H. Shimizu, *Inorg. Chem.*, 2001, **40**, 582–583; (*i*) S. K. Mäkinen, N. J. Melcer, M. Parvez and G. K. H. Shimizu, *Chem. Eur. J.*, 2001, **7**, 5176–5182; (*j*) G. K. H. Shimizu, G. D. Enright, C. I. Ratcliffe, K. F. Preston, J. L. Reid and J. A. Ripmeester, *Chem. Commun.*, 1999, 1485–1486; (*k*) G. K. H. Shimizu, G. D. Enright, C. I. Ratcliffe and J. A. Ripmeester, *Chem. Commun.*, 1999, 461–462; (*l*) G. K. H. Shimizu, G. D. Enright, C. I. Ratcliffe, G. S. Rego, J. L. Reid and J. A. Ripmeester, *Chem. Mater.*, 1998, **10**, 3282–3283.

9 (*a*) J. Cai, C.-H. Chen, C.-Z. Liao, X.-L. Feng and X.-M. Chen, *Acta Crystallogr., Sect. B*, 2001, **57**, 520–530; (*b*) J. Cai, C.-H. Chen, C.-Z. Liao, J.-H. Yao, X.-P. Hu and X.-M. Chen, *J. Chem. Soc., Dalton Trans.*, 2001, 1137–1142; (*c*) J. Cai, C.-H. Chen, X.-L. Feng, C.-Z. Liao and X.-M. Chen, *J. Chem. Soc., Dalton Trans.*, 2001, 2370–2375.

10 (*a*) B. J. Gunderman, I. D. Kabell, P. J. Squattrito and S. N. Dubey, *Inorg. Chim. Acta*, 1997, **258**, 237–246; (*b*) B. J. Gunderman and P. J. Squattrito, *Inorg. Chem.*, 1995, **34**, 2399–2406; (*c*) B. J. Gunderman and P. J. Squattrito, *Inorg. Chem.*, 1994, **33**, 2924–2931; (*d*) A. Shubnell, E. Kosnic and P. J. Squattrito, *Inorg. Chim. Acta*, 1994, **216**, 101–112; (*e*) E. J. Kosnic, E. L. McClymont, R. A. Hodder and P. J. Squattrito, *Inorg. Chim. Acta*, 1992, **201**, 143–151.

11 (*a*) A. Chatterjee, E. N. Maslen and K. J. Watson, *Acta Crystallogr., Sect. B*, 1988, **44**, 381–386; (*b*) W. Frank, G. J. Reiss and J. Schneider, *Angew. Chem., Int. Ed. Engl.*, 1995, **34**, 2416–2417; (*c*) K. R. Fewings, P. C. Junk, D. Georganopoulou, P. D. Prince and J. W. Steed, *Polyhedron*, 2001, **20**, 643–649.

12 A. Gavezzotti, *Acc. Chem. Res.*, 1994, **27**, 309–314; J. D. Dunitz, *Chem. Commun.*, 2003, 545–548.

13 (*a*) M. D. Hollingsworth, *Science*, 2002, **295**, 2410–2413; (*b*) G. R. Desiraju, *Nature*, 2001, **412**, 397–400; (*c*) D. B. Mitzi, *J. Chem. Soc., Dalton Trans.*, 2001, 1–12; (*d*) *J. Chem. Soc., Dalton Trans.*, 2000, Number 21, special issue on inorganic crystal engineering; (*e*) *Coord. Chem. Rev.*, 1999, 183, issue dedicated to crystal engineering; (*f*) D. Braga and F. Grepioni, *Acc. Chem. Res.*, 2000, **33**, 601–608; (*g*) J. D. Dunitz and A. Gavezzotti, *Acc. Chem. Res.*, 1999, **32**, 677–684; (*h*) D. Braga and F. Grepioni, *J. Chem. Soc., Dalton Trans.*, 1999, 1–8; (*i*) D. Braga, F. Grepioni and G. R. Desiraju, *Chem. Rev.*, 1998, **98**, 1375–1405; (*j*) G. R. Desiraju, *Chem. Commun.*, 1997, 1475–1482; (*k*) G. R. Desiraju, *Angew. Chem., Int. Ed. Engl.*, 1995, **34**, 2311–2327.

14 T. Steiner, *Angew. Chem., Int. Ed. Engl.*, 2002, **41**, 48–76; G. R. Desiraju, *Acc. Chem. Res.*, 2002, **35**, 565–573; L. M. Epstein and E. S. Shubina, *Coord. Chem. Rev.*, 2002, **231**, 165–181; M. J. Calhorda, *Chem. Commun.*, 2000, 801–809; G. R. Desiraju, *J. Chem. Soc., Dalton Trans.*, 2000, 3745–3751; I. Alkorta, I. Rozas and J. Elguero, *Chem. Soc. Rev.*, 1998, **27**, 163–170; T. Steiner, *Chem. Commun.*, 1997, 727–734; C. B. Aakeröy and K. R. Seddon, *Chem. Soc. Rev.*, 1993, **22**, 397–407; G. R. Desiraju, *Acc. Chem. Res.*, 1991, **24**, 290–296.

15 P. Metrangolo and G. Resnati, *Chem. Eur. J.*, 2001, **7**, 2511–2519; J. A. R. P. Sarma and G. R. Desiraju, *Acc. Chem. Res.*, 1986, **19**, 222–228; A. C. Legon, *Chem. Eur. J.*, 1998, **4**, 1890–1897; A. C. Legon, *Angew. Chem., Int. Ed.*, 1999, **38**, 2687–2714; O. Hassel, *Science*, 1970, **170**, 497–502; H. A. Bent, *Chem. Rev.*, 1968, **68**, 587–648.

16 (*a*) C. A. Hunter, K. R. Lawson, J. Perkins and C. J. Urch, *Perkin Trans. 2*, 2001, 651–669; (*b*) C. Janiak, *J. Chem. Soc., Dalton Trans.*, 2000, 3885–3896; (*c*) H. Suezawa, T. Yoshida, Y. Umezawa, S. Tsuboyama and M. Nishio, *Eur. J. Inorg. Chem.*, 2002, 3148–3151; (*d*) H. Takahashi, S. Tsuboyama, Y. Umezawa, K. Honda and M. Nishio, *Tetrahedron*, 2000, **56**, 6185–6191; (*e*) J. C. Ma and D. A. Dougherty, *Chem. Rev.*, 1997, **97**, 1303–1324; (*f*) D. Quiñonero, C. Garau, C. Rotger, A. Frontera, P. Ballester, A. Costa and P. M. Deyà, *Angew. Chem., Int. Ed.*, 2002, **41**, 3389–3392; (*g*) M. Mascal, A. Armstrong and M. D. Bartberger, *J. Am. Chem. Soc.*, 2002, **124**, 6274–6276.

17 W. J. Hunks, M. C. Jennings and R. J. Puddephatt, *Inorg. Chem.*, 2002, **41**, 4590–4598 and references therein; H. Schmidbaur, *Nature*, 2001, **413**, 31–33; P. Pyykkö, *Chem. Rev.*, 1997, **97**, 597–636; S. S. Pathaneni and G. R. Desiraju, *J. Chem. Soc., Dalton Trans.*, 1993, 319–322.

18 T. Laube, *Chem. Rev.*, 1998, **98**, 1277–1312; N. J. Turro, *Chem. Commun.*, 2002, 2279–2292; P. Hobza, V. Špirko, H. L. Selzle and E. W. Schlag, *J. Phys. Chem. A*, 1998, **102**, 2501–2504; P. Hobza, V. Špirko, Z. Havlas, K. Buchhold, B. Reinmann, H.-D. Barth and B. Brutschy, *Chem. Phys. Lett.*, 1999, **299**, 180–186.

19 C. S. Rondestvedt, Jr. and P. K. Chang, *J. Am. Chem. Soc.*, 1955, **77**, 6532–6540.

20 P. R. Morris, U. S. Patent 1972, US 3,632,600.

21 H. R. Matthews, L. C. Bucke and A. G. Blackman, *Inorg. Chim. Acta*, 1998, **277**, 89–97.

22 R. M. Silverstein, G. C. Bassler and T. C. Morrill, *Spectrometric identification of organic compounds*, 4th edn., John Wiley, New York, 1981, pp. 132–133.

23 R. D. Shannon, *Acta Crystallogr., Sect. A*, 1976, **32**, 751–767.

24 (*a*) Recent examples of supramolecular structures involving aromatic interactions between pyrazole rings : D. L. Reger, R. F. Semeniuc and M. D. Smith, *Dalton Trans.*, 2002, 476–477; (*b*) D. L. Reger, R. F. Semeniuc and M. D. Smith, *Inorg. Chem.*, 2001, **40**, 6545–6546.

25 A. R. Kennedy, M. P. Hughes, M. L. Monaghan, E. Staunton, S. J. Teat and W. E. Smith, *J. Chem. Soc., Dalton Trans.*, 2001, 2199–2205.

26 F. H. Allen and O. Kennard, *Chem. Des. Autom. News*, 1993, **8**, 31–37 (ConQuest version 1.4, 2002).

27 (*a*) Data Collection: SMART-NT Software Reference Manual, version 5.0, BrukerAXS, Inc. Madison, WI, 1998, 53719-1173; (*b*) Data Reduction: SAINT-NT Software Reference Manual, version 4.0, Bruker AXS, Inc., Madison, WI, 1996, 53719-1173; (*c*) G. M. Sheldrick, SHELXTL-NT, version 5.1, Bruker AXS, Inc., Madison, WI, 1999, 53719-1173.